CRYSTAL GROWTH & DESIGN

Subscriber access provided by GRIFFITH UNIVERSITY

Article

Evaluation of the role of isostructurality in fluorinated phenyl benzoates

Dhananjay Dey, and Deepak Chopra

Cryst. Growth Des., **Just Accepted Manuscript** • DOI: 10.1021/acs.cgd.7b00421 • Publication Date (Web): 07 Sep 2017

Downloaded from http://pubs.acs.org on September 8, 2017

Just Accepted

"Just Accepted" manuscripts have been peer-reviewed and accepted for publication. They are posted online prior to technical editing, formatting for publication and author proofing. The American Chemical Society provides "Just Accepted" as a free service to the research community to expedite the dissemination of scientific material as soon as possible after acceptance. "Just Accepted" manuscripts appear in full in PDF format accompanied by an HTML abstract. "Just Accepted" manuscripts have been fully peer reviewed, but should not be considered the official version of record. They are accessible to all readers and citable by the Digital Object Identifier (DOI®). "Just Accepted" is an optional service offered to authors. Therefore, the "Just Accepted" Web site may not include all articles that will be published in the journal. After a manuscript is technically edited and formatted, it will be removed from the "Just Accepted" Web site and published as an ASAP article. Note that technical editing may introduce minor changes to the manuscript text and/or graphics which could affect content, and all legal disclaimers and ethical guidelines that apply to the journal pertain. ACS cannot be held responsible for errors or consequences arising from the use of information contained in these "Just Accepted" manuscripts.

ACS Publications

Crystal Growth & Design is published by the American Chemical Society. 1155 Sixteenth Street N.W., Washington, DC 20036

Published by American Chemical Society. Copyright © American Chemical Society. However, no copyright claim is made to original U.S. Government works, or works produced by employees of any Commonwealth realm Crown government in the course of their duties.

Evaluation of the role of isostructurality in fluorinated phenyl benzoates

Dhananjay Dey[a], *Deepak Chopra*[a]*

[a]*Crystallography and Crystal Chemistry Laboratory, Department of Chemistry, Indian Institute of Science Education and Research Bhopal, Bhauri, Bhopal-462066, Madhya Pradesh, India.*

ABSTRACT

In this report, the occurrence of 3D, 2D and 1D isostructurality in phenyl benzoate (D00) and their fluorinated analogues was investigated in terms of their molecular assembly in solid state structures. One-dimensional C-H···O=C chain is observed as a robust motif (~ -21 kJ/mol) in the formation of the supramolecular architectures in these isostructural compounds. The isomorphous crystal structures exhibit 3D isostructurality or vice-versa. The crystal packing shows that weak intermolecular C-H···F, C-H···O, C-H···π interactions and π···π stacking are the main contributors providing stability towards the crystal lattice. The nature and energetics of all the geometrically or energetically equivalent building blocks associated with similar or different intermolecular interactions delineate the role of different molecular pairs in the crystal structures. The fingerprint plots of the isostructural set of crystal structures helps to understand the similarities and the differences in the various interatomic contacts. A comparison of these crystal structures with the fluorinated *N*-phenyl benzamides shows the change in supramolecular assembly in terms of intermolecular interactions as well as the lattice energy due to the participation of a strong donor (N-H).

1. INTRODUCTION

The importance of organic fluorine [1-2] in supramolecular assembly is well-recognized, especially in the field of crystal engineering [3-5]. Fluorinated compounds have an impact on the chemical reactivity and the biological activity when compared to the non-fluorianted derivatives [6-7]. The substitution of hydrogen atom/atoms with fluorine changes the chemical reactivity in various drugs and pharmaceuticals [8]. Fluorine can generate different types of supramolecular motifs to build the crystal lattice *via* intermolecular C-H···F [9-11], C-F···F [12-13] and C-F···π [14] interactions in the absence or presence of any strong donor [15]. The major exercise in crystal engineering is dedicated towards the achievement of desired features utilizing the various intermolecular interactions *via* the mutual assembly of the molecules in the crystal lattice [16-18]. The existence of two different crystal structures with 3D or 2D or 1D structural similarity in their molecular arrangements is called isostructurality [18-20]. The structural similarities in the molecular arrangement between the two crystal structures can be shown as 1D molecular chain, 2D layer and 3D supramolecular construct [18, 21]. Two crystal structures can be isomorphous [22-23] with similar space group and identical unit cell parameters. In most of the cases, the isomorphous solid-state structures show 3D isostructurality [20]. Furthermore, it is not necessary that crystal structures with 1D and 2D isostructurality will be isomorphous. Nath *et al* have discussed the isomorphous and isostructural behaviour in the crystal structures of fuchsones compounds on account of chloro-methyl exchange [23]. The investigations on isostructurality and their relevant applications are also of immense interest [20, 24-28]. Furthermore, isostructurality can affect the mechanical property of the material i.e. two isostructural (need not be isomorphous) compounds can show different mechanical properties [29-30]. The occurrence of isostructurality is very common in similar type compounds with equivalent functionalities like -H, -CH_3, -F, -Cl, -Br and I [31-32].

Our recent study, has established the occurrence of 3D isostructurality in the presence of strong hydrogen bonds, namely N-H···N, associated with the presence of weak C-H···N [33], C-H···F, C-H···π [34] interactions and π···π stacking in fluorinated *N*-phenyl benzimidamide compounds [24]. Previously, the investigation on the crystal structures of 4,5′-substituted benzenesulfonamido-2-pyridines shows the robustness of the supramolecular architectures having centrosymmetric N-H···N dimers which lead to the existence of 3D isostructurality [35]. It has been already observed that weak intermolecular interactions play an important role in the formation of the crystal lattice in *in situ* cryocrystallized fluorinated benzoyl chlorides [36], wherein the columnar molecular array, stabilized via the primary building block (involving π···π stacking), are interlinked *via* the secondary supramolecular motifs like C–H···O/F/Cl interactions [37] and halogen···halogen contacts. Thus, our aim of this work was to investigate the isostructurality (3D, 2D and 1D) in the absence of any strong hydrogen bond in fluorinated phenyl benzoates (FPB) where the crystal packing is governed mainly by the weak intermolecular interactions.

2. EXPERIMENTAL

Phenyl benzoate and their fluoro-derivatives (**Scheme 1**) have been synthesized and characterized *via* ^{1}H-NMR, FTIR spectroscopy, differential scanning calorimetry (DSC) and powder X-ray diffraction (**Figures S1-S11**). The synthetic procedure was undertaken using well established procedures [38] and provided in the ESI.

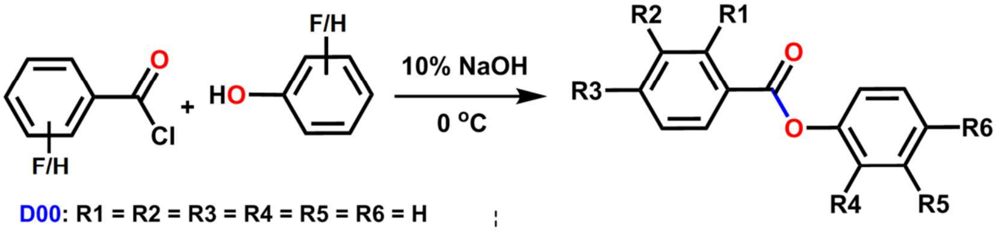

D00: R1 = R2 = R3 = R4 = R5 = R6 = H
D01: R1= F, R2 = R3 = R4 = R5 = R6 = H
D02: R2 = F, R1 = R3 = R4 = R5 = R6 = H
D03: R3 = F, R1 = R2 = R4 = R5 = R6 = H
D10: R4 = F, R1 = R2 = R3 = R5 = R6 = H
D20: R5 = F, R1 = R2 = R3 = R4 = R6 = H

D21: R5 = R1 = F, R2 = R3 = R4 = R6 = H
D22: R5 = R2 = F, R1 = R3 = R4 = R6 = H
D31: R6 = R1 = F, R2 = R3 = R4 = R5 = H
D32: R6 = R2 = F, R1 = R3 = R4 = R5 = H
D33: R6 = R3 = F, R1 = R2 = R4 = R5 = H

Scheme 1

2.1. Crystal Growth

The crystallization of the pure synthesized compounds has been performed *via* solvent evaporation method in different polar, non-polar and polar-non polar mixture of solvents (HPLC grade) at various conditions (at temperatures 25°C and 4°C). The slow evaporation method has been applied to get high-quality single crystals. In most of the cases, the crystals were obtained from (dichloromethane and hexane mixture), (acetone and hexane mixture), cyclohexane, and methanol solvent systems. For the low melting solid D22 (the melting point is 32.8ºC), we have used *in situ* cryocrystallization [39] technique using OHCD to crystallize this compound. The details of *in situ* cryocrystallization technique are available in the ESI of our previous study [40].

2.2. Crystal Structure Determination and Modelling of Disorder

The crystal structures of the unsubstituted phenyl benzoate D00 [41-42] and FPBs namely D01 [42], D02 [43] and D03 [42] are already reported in the literature. The reported crystal data were collected at 298K, and hence we have again re-determined the crystal structures of D00, D01, D02 and D03 at 100K. The details of crystal structure refinement are discussed in the ESI. In the case of $P2_1$ and $P2_12_12_1$ space group, the inversion twin refinement (refined as two-component twin) has been performed using BASF command. **Table S1** lists the details of the structure refinement parameters for all the FPBs. The *ORTEP*s of all the FPBs with the atom-numbering are shown in **Figure S12**. The occupancies of the disordered fluorine atom (connected with the carbon atom in the *ortho* and *meta* positions on the substituted benzene ring) at the two positions were refined by using the PART command in SHELXL 2014 [44], namely F1A & F1B and F2A & F2B ('A' part contains the higher occupancy and 'B" part corresponds to the lower occupancy for that atom). The atomic positions of the carbon atom (A and B) of the disordered benzene ring were fixed with EXYZ command and the anisotropic displacement parameter for these two sites (A and B) of the carbon and fluorine atom was fixed using the EADP command. In case of D20 (F1A and F1B), D22 (F2A and F2B), D31 (F1A and F1B) and D32 (F1A and F1B), the fluorine atoms are positionally disordered. The role of the disordered fluorine in the crystal packing has been explored previously in the literature [45-46] where the fluorine atom exhibits positional disorder mainly in case of *ortho* and *meta* substituted *N*-phenyl benzamides. In the course of all computational investigations, the atomic coordinates (with normalized C-H distance) of the major conformer (PART A) were considered.

3. RESULT AND DISCUSSION

In case of D01, D21 and D31, there is the formation of an intramolecular short C-F···O-C contact (**Figure S12**) primarily when the fluorine atom is attached to the *ortho* carbon atom of the substituted benzene ring (C1 > C6). The intramolecular F···O distances are 2.694(2) Å in D01, 2.679 (2) Å in D21 and 2.559(2) Å in D31. The torsion angles present in the structure and the dihedral angle between the two substituted benzene rings are listed in **Table S2**. All the ten crystal structures have been analyzed based on their supramolecular architectures as well as the presence of geometrically and energetically similar structural building blocks present in the crystal packing. The intermolecular interaction energy and their components (Coulombic, polarization, dispersion and repulsion) obtained from *PIXEL* method [47-48] are given in ESI. Cg1 and Cg2, mentioned in the entire discussion, are the centroids of corresponding benzene rings C1 > C6 and C7 > C12 respectively.

3.1. Structural Similarity Analysis

The structural similarities between unsubstituted phenyl benzoate (D00) and fluorinated analogues have been investigated using *XPac* 2.0.2 program (version 2.0.2) [49-51], introduced by Gelbrich and co-workers. All the atomic coordinates (in crystal geometry) except the hydrogen and fluorine atoms, were considered for the *XPac* analysis. This method helps to identify the supramolecular construct and the extent of crystal packing similarity (called as *dissimilarity index* x) in three dimensional (3D) or two dimensional (2D) or one dimensional (1D) molecular arrangement between two crystal structures. It also provides quantitative estimates to the dissimilarity parameters, namely, the stretch parameter (the magnitude by which the crystal packing of one structure is stretched in comparison to the crystal packing of the other structure), the extent of the change in angles and planes between two crystal structures. From the analysis, it is observed that some structures shows 3D crystal packing similarity, some are related with each other *via* 2D similarity and in the maximum cases, 1D (**Figure S13**) structural similarity is observed. This feature is due to the presence of a C-H··O chain which is present in the parent structure D00. **Figure 1** and **Table 1** shows the overall structural similarity amongst these eleven crystal structures. The 3D and 2D isostructural combinations are shown with the red color box and indigo color box respectively. The green color box indicates the similar combination (100% similarity) between structures such as D00-D00, D01-D01 etc. The yellow color box shows the 1D packing similarities with C-H···O chain. From the analysis, it is observed that the dissimilarity index value is in the range of 2.5-5.3, 1.6-9.9 and 4.0-12.6 for 3D, 2D and 1D isostructural pair of crystal structures respectively. In most of the 1D isostructural cases, inspite of the high values of the "dissimilarity index", the similarities do exist on account of the presence of the common building block consisting of a 1D C-H···O chain.

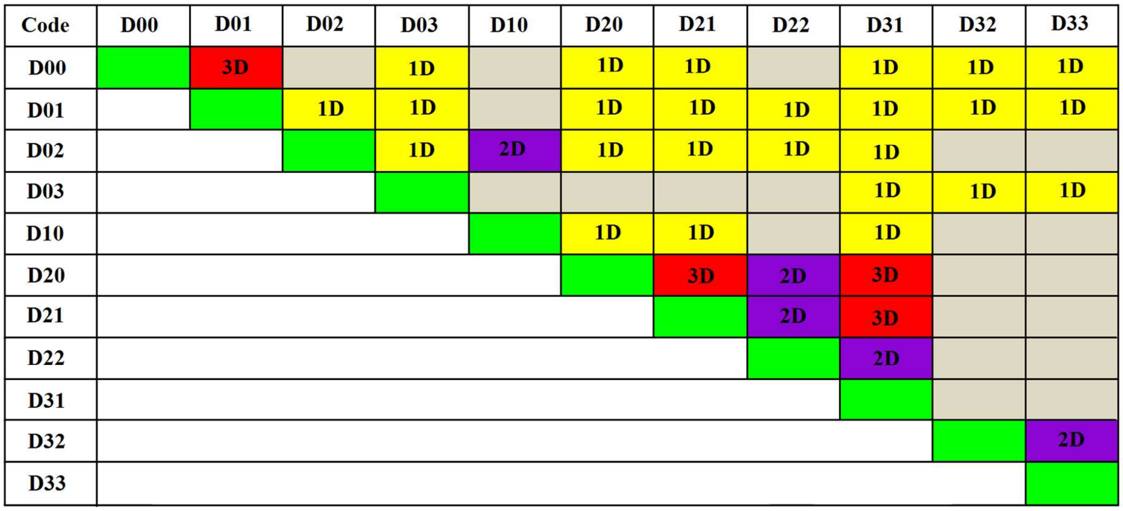

Code	D00	D01	D02	D03	D10	D20	D21	D22	D31	D32	D33
D00	🟩	3D	▨	1D	▨	1D	1D	▨	1D	1D	1D
D01		🟩	1D	1D	▨	1D	1D	1D	1D	1D	1D
D02			🟩	1D	2D	1D	1D	1D	1D	▨	▨
D03				🟩	▨	▨	▨	▨	1D	1D	1D
D10					🟩	1D	1D	▨	1D	▨	▨
D20						🟩	3D	2D	3D	▨	▨
D21							🟩	2D	3D	▨	▨
D22								🟩	2D	▨	▨
D31									🟩	▨	▨
D32										🟩	2D
D33											🟩

Figure 1. The map containing the structural similarity (3D, 2D, 1D and no similarity) for the eleven crystal structures of FPB [the green color indicates the similar combination].

Table 1. The structural similarity (3D, 2D and 1D) parameters for the isostructural FPBs

Combination		Dissimilarity index (x)	Stretch Parameter (Å)	Δ a (°)	Δ p (°)
3D Isostructurality					
D00	D01	4.5	0.15	1.9	4.1
D20	D21	2.5	0.15	1.2	2.1

D20	**D31**	**4.5**	**0.12**	**1.8**	**4.0**
D21	**D31**	**5.3**	**0.19**	**2.3**	**4.7**
2D Isostructurality					
D22	**D20**	**4.6**	**0.16**	**2.0**	**4.1**
D22	**D21**	**5.2**	**0.20**	**2.3**	**5.7**
D22	**D31**	**4.3**	**0.23**	**2.4**	**3.6**
D32	**D33**	**1.6**	**0.06**	**0.7**	**1.5**
D02	**D10**	**9.9**	**0.38**	**5.4**	**7.8**
1D Isostructurality (C-H···O chain)					
D00	**D03**	**4.0**	**0.12**	**1.5**	**3.7**
D00	**D20**	**12.9**	**0.59**	**10.1**	**8.0**
D00	**D31**	**11.5**	**0.40**	**9.0**	**7.2**
D00	**D32**	**9.4**	**0.12**	**6.2**	**7.0**
D00	**D33**	**8.8**	**0.09**	**5.9**	**6.5**
D01	**D02**	**7.3**	**0.03**	**5.4**	**4.4**
D01	**D03**	**7.2**	**0.02**	**3.5**	**6.3**
D01	**D20**	**11.8**	**0.49**	**8.6**	**8.0**
D01	**D21**	**12.1**	**0.61**	**8.9**	**8.2**
D01	**D22**	**12.7**	**0.58**	**9.9**	**7.9**
D01	**D31**	**9.9**	**0.30**	**7.4**	**6.6**
D01	**D32**	**12.6**	**0.02**	**8.2**	**9.6**
D01	**D33**	**12.0**	**0.01**	**7.9**	**9.1**
D02	**D03**	**11.2**	**0.01**	**8.2**	**7.6**
D02	**D20**	**7.5**	**0.46**	**3.9**	**6.4**
D02	**D21**	**8.1**	**0.58**	**4.4**	**6.4**
D02	**D22**	**6.8**	**0.55**	**4.8**	**4.9**
D02	**D31**	**4.9**	**0.27**	**2.4**	**4.2**
D03	**D31**	**13.7**	**0.28**	**10.1**	**9.2**
D03	**D32**	**6.4**	**0.00**	**4.9**	**4.1**
D03	**D33**	**5.9**	**0.03**	**4.7**	**3.5**
D10	**D20**	**9.2**	**0.02**	**4.8**	**7.8**
D10	**D21**	**8.9**	**0.14**	**4.7**	**7.7**
D10	**D31**	**8.0**	**0.17**	**5.4**	**5.9**

3.2. 3D isostructurality between D00 and D01

The crystal structures of D00 and D01 are isomorphous in monoclinic $P2_1/c$ space group with Z = 4. In both cases, two molecules (associated with C-H···π and C-H···O interactions) together act as a single unit (sandwich) and these units are arranged in a herringbone pattern down the *bc* plane (**Figure 2a** and **2b**). Along *a* axis the molecules form C-H···O chain, (**Figure S13**) involving carbonyl oxygen (O2) and the aromatic hydrogen atom (H12). A comparison between the crystal structures D00 and D01 reveals the presence of 3D supramolecular construct (**Figure 2c**) with the dissimilarity index value of 4.5. It is observed that there is no change in the supramolecular construct on incorporation of the fluorine atom at the *ortho* position on the substituted benzene ring (C1 > C6). The stabilization energies for all the molecular pairs (associated with the various intermolecular interactions) involved in

3D isostructural D00-D01 were determined using *PIXEL* method. **Table S3** lists all the extracted molecular pairs (with the decreasing order of stabilization energy). Each molecular pair present in D00 is associated in a similar manner with a molecular pair of D01 (presence of similar or different interactions). **Figure 3** shows the equivalent building blocks present between D00 and D01. The strongest molecular pairs [D00-I (-24.1 kJ/mol)/D01-I (-24.8 kJ/mol)] are associated with the weak intermolecular C8-H8···O1 and C9-H9···π interactions (**Figure 3a**). In addition, the 3D isostructural compound D00-D01 contains the 1D C-H···O chain (molecular pair II) with stabilization energy of ~ -21 kJ/mol, having 31-33% electrostatic contribution (**Figure S14**) to the total stabilization. The maximum equivalent molecular pairs (**Figure 3**) [D00-I/D01-I, D00-II/D01-II, D00-III (-19.8kJ/mol) /D01-III (-21.1kJ/mol), D00-IV (-13.9kJ/mol)/D01-IV (-15.2kJ/mol) , D00-V (-10.6 kJ/mol)/D01-VIII (-10.4 kJ/mol), D00-VI (-10.3 kJ/mol) / D01-VII (-10.8 kJ/mol) and D00-VIII (-6.3 kJ/mol)/ D01-IX (-7.4kJ/mol)] are isoenergetic, except in the case of D00-VII/D01-V and D00-IX/D01-VI.

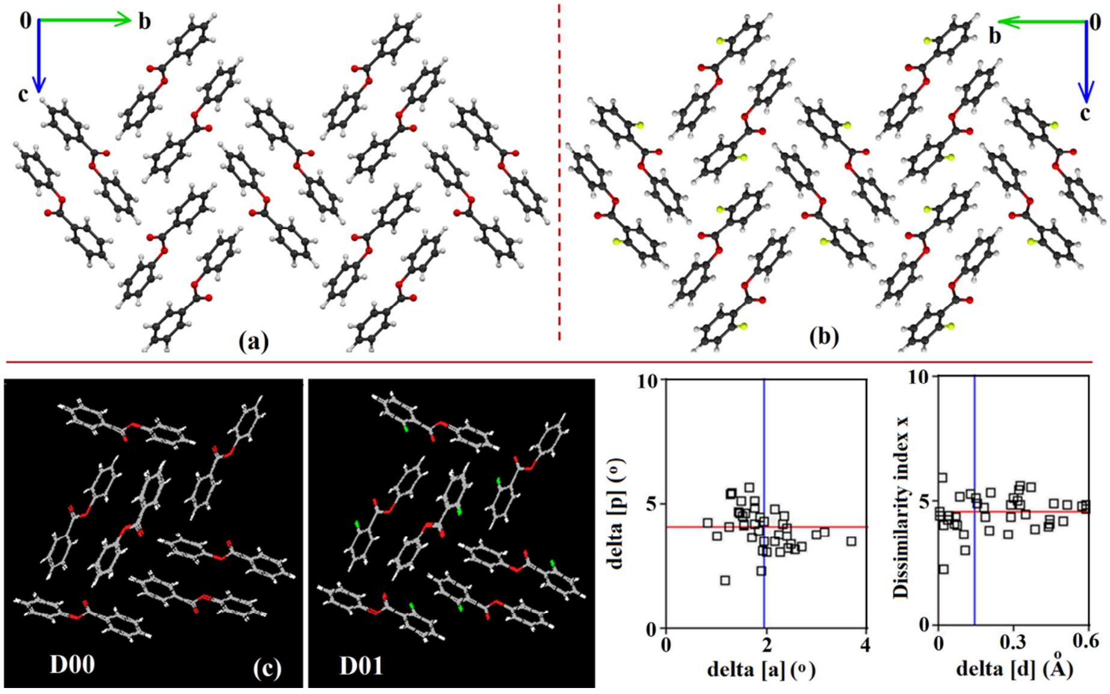

Figure 2. The molecular arrangement in (a) D00 down the *bc* plane and (b) D01 down the *bc* plane; (c) 3D supramolecular constructs obtained from *XPac* analysis for D00-D01.

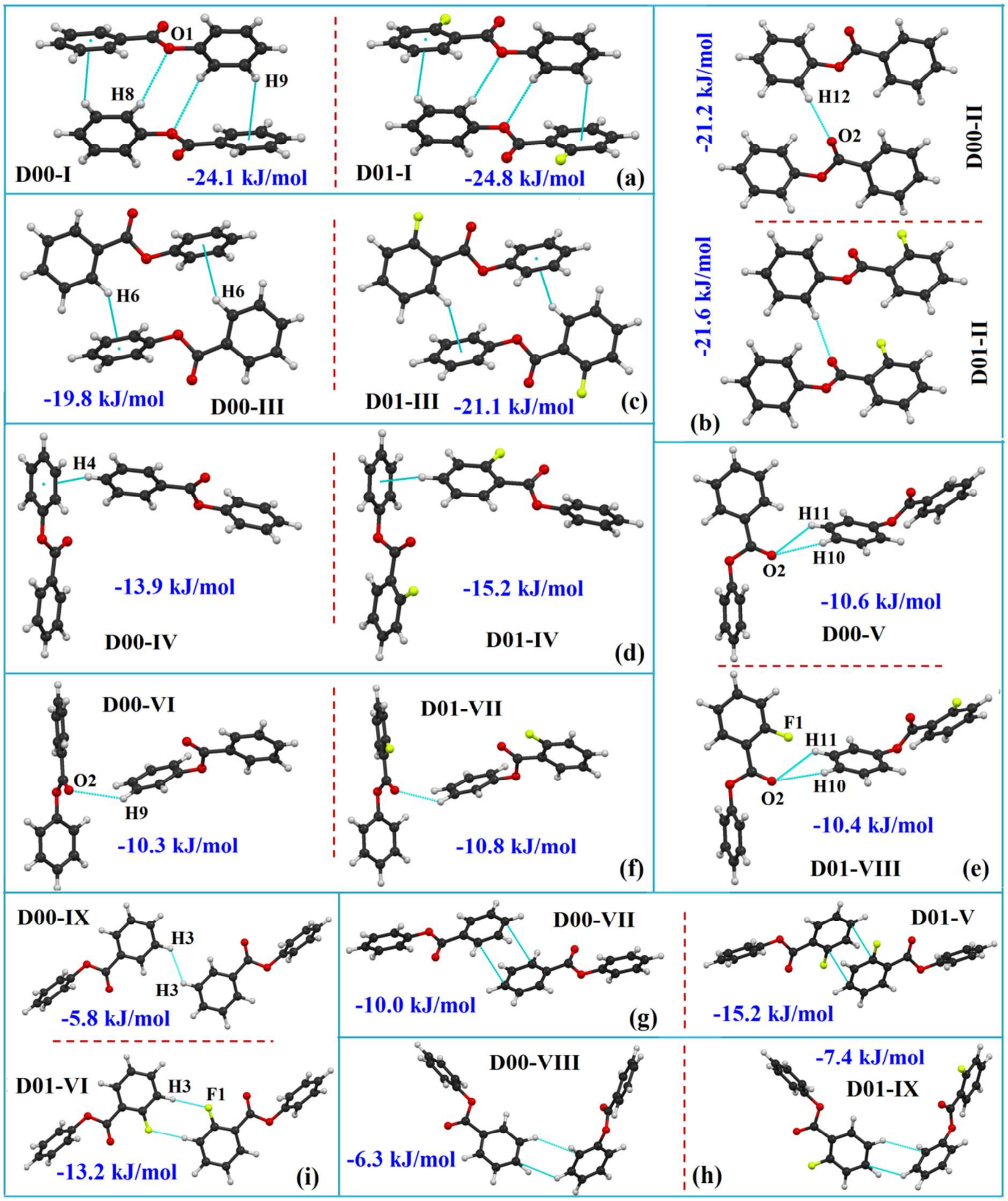

Figure 3. The equivalent molecular pairs with their stabilization energies for the 3D isostructural compounds D00-D01.

The energetic contribution (electrostatics and dispersion) towards the total stabilization for all the equivalent molecular pairs of isostructural compound D00-D01 is shown in **Figure S14**. In the case of D00-IX (-5.8 kJ/mol), only H3···H3 contact (2.41Å) is present whereas, in D01-VI (-15.2 kJ/mol), there is a formation of C3-H3···F1 dimer (**Figure 3i**) having short H···F [9, 52] distance (2.44Å) and high directionality (162°). Hence, the electrostatic contribution is 38% more for D01-VI in comparison to D00-IX. The π···π stacking [C4···C2 distance is 3.750Å] present in D00-VII (-10.0 kJ/mol) is more offset compared to the π···π stacking [C4···C2 distance is 3.519(2)Å] in D01-V (-15.2 kJ/mol) (**Figure 3g**). As the fluorinated benzene rings are more electron deficient, the electrostatic contribution is -4.8kJ/mol (13%) more when compared to the interaction between two unsubstituted benzene rings in D00-VII.

3.3. 3D and 2D isostructurality between D20, D21, D22 and D31

The single crystal X-ray diffraction study reveals that the crystal structures of D20, D21 and D31 (**Figure S12** and **Table S1**) are isomorphous in $P2_12_12_1$ space group with Z = 4. In all three cases, the molecules are assembled in a similar type of zigzag fashion (**Figure S15**) down the *bc* plane. *XPac* analysis shows the presence of 3D supramolecular construct with dissimilarity index of 2.5 for D20-D21 (**Figure 4a**), 4.5 for D20-D31 (**Figure 4b**) and 5.3 for D21-D31 (**Figure 4c**). The close distribution of the data points at low angle with lower magnitude of stretch parameter in the plot of Δp vs Δa and x vs Δd, support the existence of isostructural behaviour between these three crystal structures. All the equivalent building blocks for the 3D isostructural D20-D21-D31 are shown in **Figure 5**. Interestingly, the low melting solid D22 which crystallizes in $P2_1/n$ with Z = 4, is also related to D20, D21 and D31 with 2D structural similarity with the dissimilarity index of 4.6 for D22-D20 (**Figure S16**), 5.2 for D22-D21 (**Figure S17)** and 4.3 for D22-D31 (**Figure S18**). **Table S4** lists all the possible molecular pairs with their interaction energies for the crystal structures of D20, D21 D22 and D31.

The crystal packing of D22 (**Figure S19**) shows the zigzag molecular sheet associated with C-H···F dimeric chain down the (015) and (01-5) planes. The molecular pairs and the stabilization energy for the individual pairs in D22 are shown in **Figure S20**. The one dimensional C12-H12···O2 chain [D20-I, D21-II, D31-II (**Figure 5a**) and D22-III (**Figure S20c**)] is preserved in all these four cases and the corresponding stabilization energies are in the range of -18.8 to -20.4 kJ/mol. The equivalent molecular pairs [D20-II, D21-I, D31-I (**Figure 5b**) and D22-II (**Figure S20b**) are associated with C8-H8···Cg2 and C-H···F interactions having the stabilization energy of ~ -20 kJ/mol. In the case of D20-II, D21-I and D22-II there is a formation of the intermolecular F···O contact (involving *meta* fluorine with the O1 atom) but in case of D31-I this is absent. Hence, the electrostatic contribution is ~ 7% more for D31-I as compared to the other three equivalent molecular pairs (**Figure 6**).

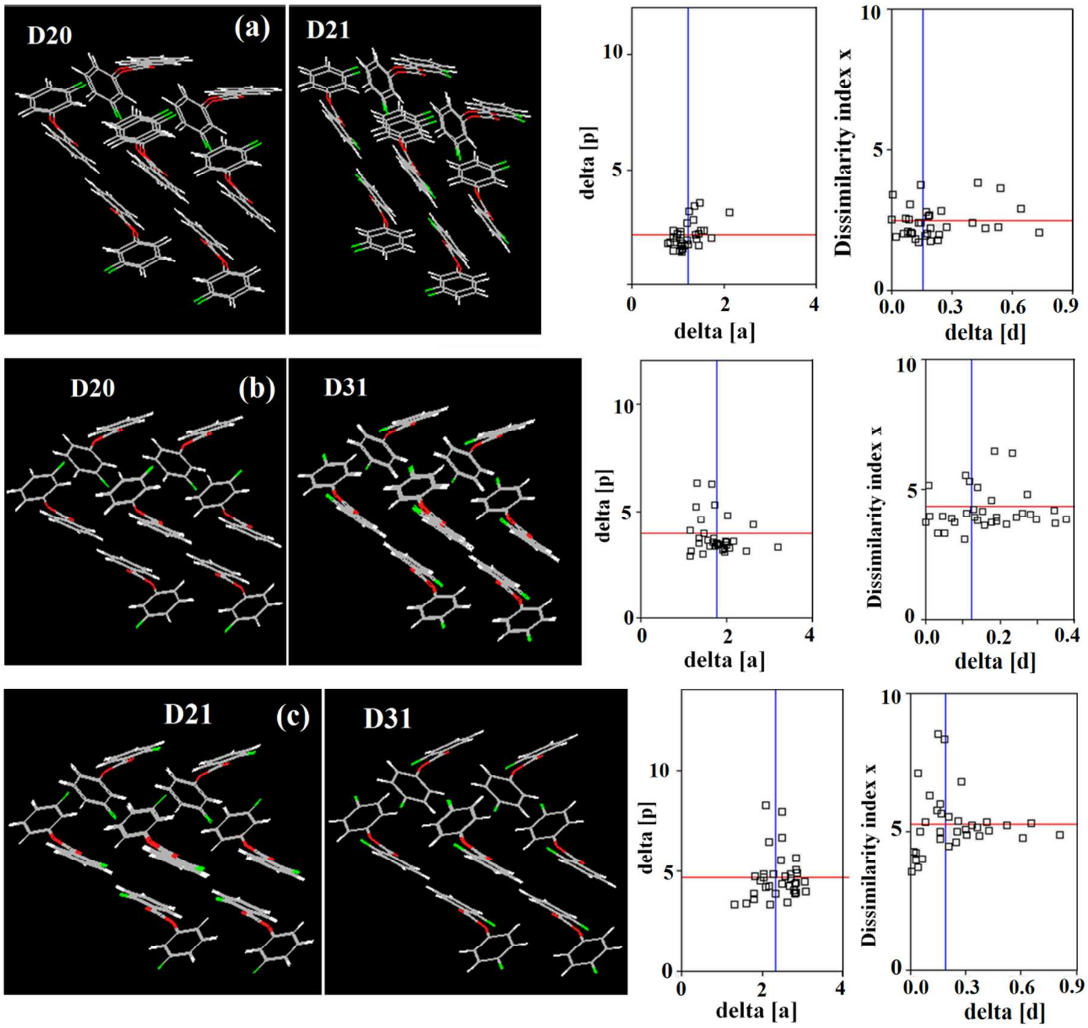

Figure 4. 3D supramolecular constructs obtained from *XPac* analysis for the isostructural pairs (a) D20-D21, (b) D20-D31 and (c) D21-D31.

The isoenergetic equivalent molecular pairs [D20-III, D21-III, D31-III (**Figure 5c**) and D22-IV (**Figure S20d**)] associated with C-H···O and C-H···π has the energy of -17.3 kJ/mol (~ 40% electrostatics and ~60% dispersion contribution). The molecular pairs IV (**Figure 5d**) of the 3D isostructural compounds D20-D21-D31 are geometrically as well as energetically (~ -13 kJ/mol) equivalent. The fifth set of equivalent molecular pairs are D20-V, D21-V and D31-V (**Figure 5e**); out of them D20-V and D31-V are isoenergetic (~ -9.0 kJ/mol) associated with intermolecular C-H···O and short H···H contact. Interestingly, D21-V (-6.9 kJ/mol) has a short ($d_{H\cdots F}$ = 2.29Å) intermolecular C-H···F contact. Hence, the electrostatic contribution for D21-V is ~ 16% more as compared to the other two equivalent pairs.

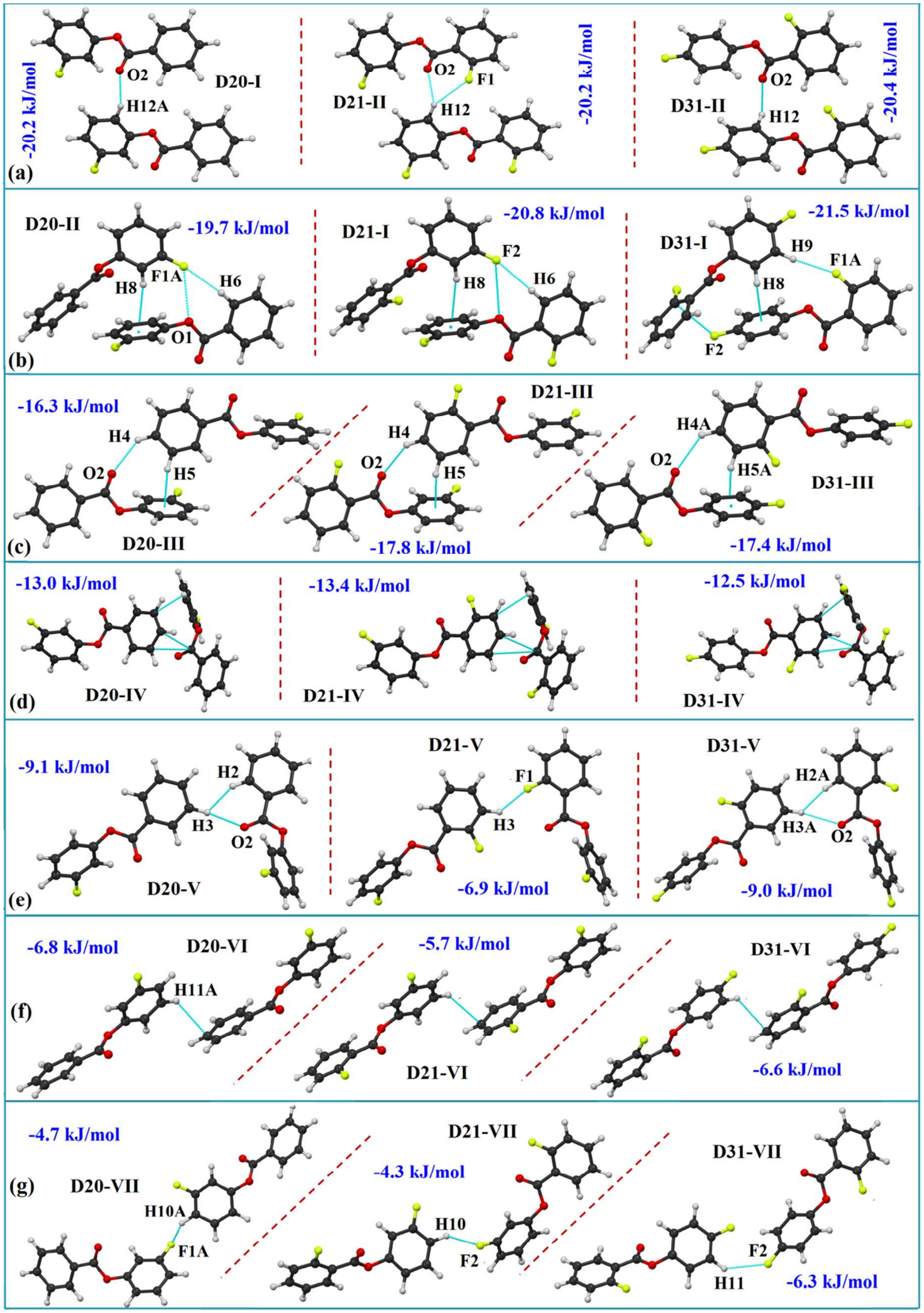

Figure 5. The equivalent molecular pairs for the 3D isostructural compounds D20-D21-D31.

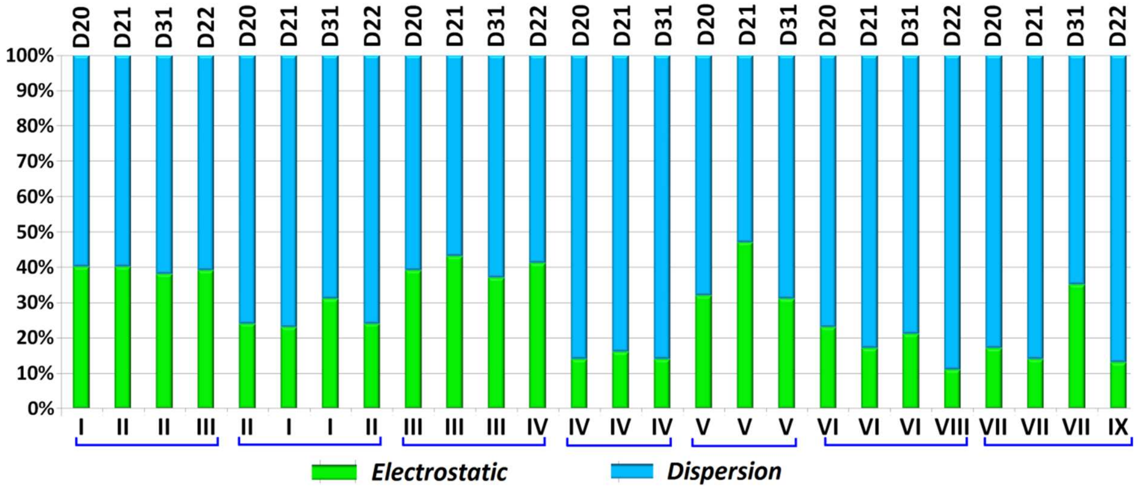

Figure 6. The energetic contributions of the equivalent molecular pairs for between D20, D21, D31 and D22.

Subsequently, the dispersion contribution for D20-V and D31-V is ~ 16% more due to the presence of short H···H contact ($d_{H\cdots H}$ ~ 2.22Å). The VI (**Figure 5f**) and VII (**Figure 5g**) molecular pairs of 3D isostructural D20-D21-D31 also geometrically equivalent with D22-VIII (-5.1 kJ/mol) (**Figure S20h**) and D22-IX (-5.1kJ/mol) (**Figure S20i**) respectively. The strongest molecular pair D22-I (-25.5 kJ/mol) (**Figure S20a**) and the other two centrosymmetric C-H···F dimers [VI (-7.9 kJ/mol) (**Figure S20e**) and VII (-5.2 kJ/mol) (**Figure S20g**)] are unique in comparison to the other molecular pairs present in D20, D21 and D31. In case of D22-VII, it is observed that the dispersion contribution (89%) to the total stabilization (-12.3kJ/mol) is very high in comparison to the electrostatic contribution (-0.3 kJ/mol) and also the repulsion component is 6 kJ/mol.

3.4. 2D structural similarity between D32 and D33

The compound D32 crystallizes in the monoclinic centrosymmetric $P2_1/c$ space group (Z = 4) whereas D33 crystallizes in the monoclinic centrosymmetric $C2/c$ space group (Z = 8). In both the cases, one fluorine atom is attached at the *para* position on the substituted benzene ring (C2 > C12) but the other fluorine atom is attached at the *meta* and *para* position of the substituted benzene ring (C1 > C6) for D32 and D33 respectively (**Figure S12**). Between these two structures, two crystallographic lattice parameters (*b* and *c*) are similar and the third one (*a* axis) is just double the other (D32). The orientation of the substituted benzene ring (C2 > C12) of one structure [rotation anti-clockwise by 54.32 (3)° from the vertical position] is different (**Figure S21**) from the other one [rotation clock-clockwise by 55.41(5)° from the vertical position]. In both the cases, the molecules were found to form a molecular sheet (**Figure S22a** and **S22b**) down the *ab* plane, wherein the zigzag C-H···F chain [C4A-H4A···F1A in D32 (**Figure S22a**) and C3-H3···F1 in D33 (**Figure S22b**)] propagates along the crystallographic *b* direction along with the 1D C-H···O (involving H12 with O2) chain in parallel. In the same sheet of D32, the 1D C-H···O chain is connected to the neighboring C-H···O chain in parallel utilizing the 2_1 screw axis *via* C-H···F interaction (involving H11 with F2) and F···F contact [2.992(1)Å] (**Figure S22a**). Whereas, there is the formation of different types of centrosymmetric C-H···F dimers (represented with different transparent color codes) which connect two parallel aligned C-H···O chains in D33 (**Figure S22b**). There is a formation of another molecular sheet [down the (0-11) plane and (011) plane in the case of D32 and D33 respectively] associated with intermolecular C-H···π, C12-H12···O1 and C-H···F interactions (**Figure S23a** and **S23b**). In the case of D32, the acidic hydrogen H2A and H5A interact with Cg1 and H8 and H11 interact with Cg2. Whereas in the case of D33, the acidic hydrogen H2 and H5 interact with Cg1 and H8 and H11 interacts with Cg2. Also, it is of interest to note that both the structures have Burgi-Dunitz type [53-54] of O=C(13)···O(2)=C interaction (interaction between carbonyl carbon with carbonyl oxygen atom) which also provides additional stability towards the crystal packing.

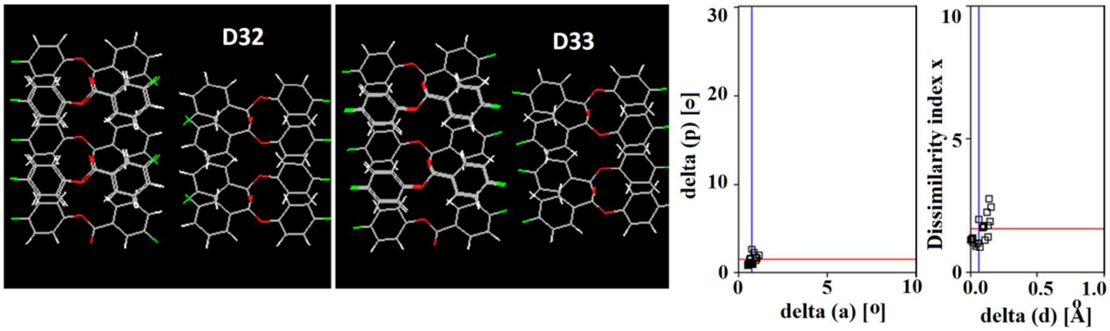

Figure 7. 2D supramolecular constructs obtained from *XPac* analysis for **D32-D33.**

The structural similarity analysis shows that these two structures are 2D isostructural (**Figure 7**) with dissimilarity index of 1.6. It has been observed that both the structures have some energetically equivalent molecular building blocks. **Table S5** lists the stabilization energies and the geometry of the interactions involved in the molecular pairs (extracted from the crystal packing) for the 2D isostructural compounds D32-D33. The molecular pairs I (-28.0/-27.6 kJ/mol), II (-23.4/-23.4 kJ/mol), III (-22.5/-22.5 kJ/mol) and VI (-4.7/-5.1 kJ/mol) of D32-D33 (**Figures 8a-d**) are isoenergetic. The orientation of the carbonyl group in D32-II is opposite to D33-II (**Figure 8b**). The electrostatic and the dispersion contributions (**Figure S24)** for the isoenergetic molecular pairs are comparable). **Figure S25** shows the molecular pairs associated with C-H···F interactions (non-centrosymmetric and centrosymmetric) for D32 and D33. These are D32-IV (-8.2 kJ/mol), D32-V (-6.3 kJ/mol), D33-IV (-7.3 kJ/mol), D33-V (-6.2 kJ/mol) and D33-VII (-4.6 kJ/mol) which also contributes further stability towards the crystal packing. It is noteworthy that fluorine-based C-H···F interactions provide a significant (21-43%) electrostatic contribution towards the stabilization of the individual molecular pairs.

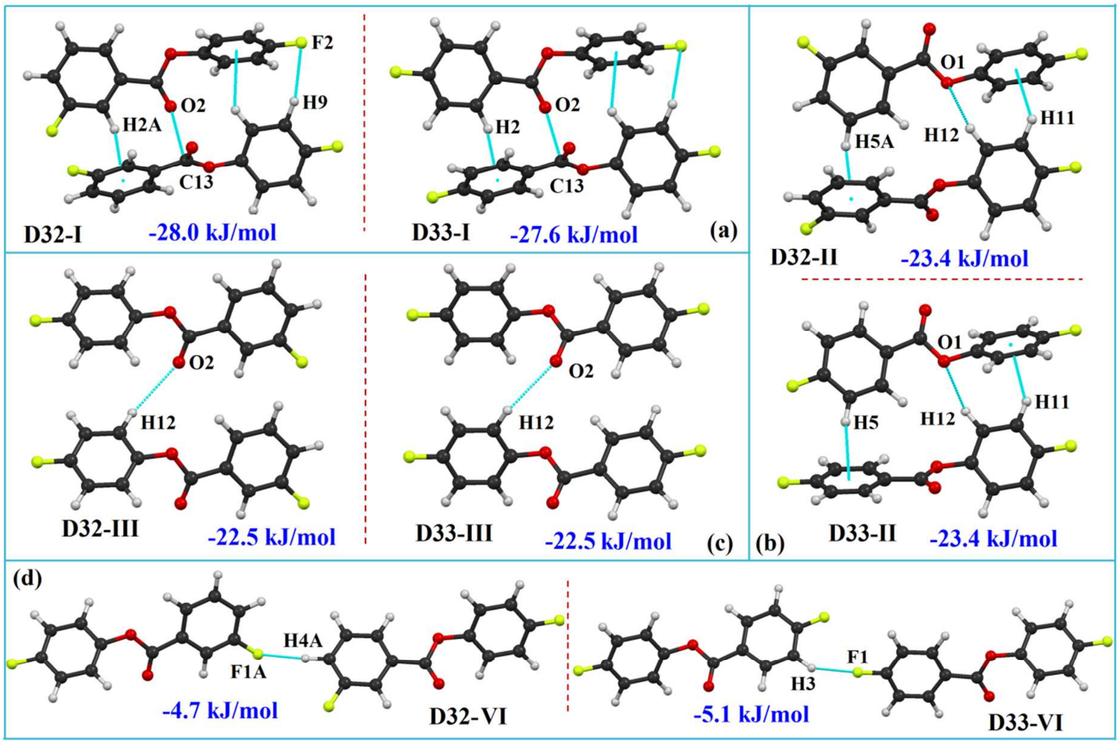

Figure 8. The equivalent molecular pairs with their stabilization energies for the 2D isostructural compounds D32-D33.

3.5. 1D and 2D Structural similarity with D02, D03, D10

Compound D02 crystallizes in $P2_12_12_1$ and has one *meta*-fluorine atom on the benzene ring (C1 > C6). It has 2D structural similarity with D10 with the dissimilarity index 9.2 (Figure S26). Also this structure has 1D structural similarity with the other structures (**Table 1**), namely D03, D20, D21, D22 and D31 due to the presence of the C12-H12···O2 chain (**Figure 9a**) having the energy range of -18.9 to -21.8 kJ/mol, wherein the electrostatic contribution is the range of 29-42% and the dispersion contribution is the range of 58-71%. **Table S6** lists all the possible molecular pairs for D02, D03 and D10. There is a formation of another molecular sheet (**Figure 9b**) down the *bc* plane normal to the C12-H12···O2 chain (*ac* plane). This sheet is associated with molecular building blocks II (-20.6 kJ/mol), III (-17.2kJ/mol), IV (-16.1 kJ/mol) and VI (-5.4 kJ/mol). The molecular pairs II [associated with C-H···F and C-H···π interaction] connect with each other *via* C3-H3···O2 along *a* direction and with the molecular pairs III (involving C10-H10···O2 and C9-H9···Cg1) and VI (involving F1 with H10) along the *c* direction. The molecular pair III is isoenergetic with the equivalent molecular pairs D20-III, D21-III, D31-III and D22-IV. In addition to that, the D02-V (involving H11 with C9; -9.1kJ/mol) molecular pair also contributes towards the stabilization in the crystal packing.

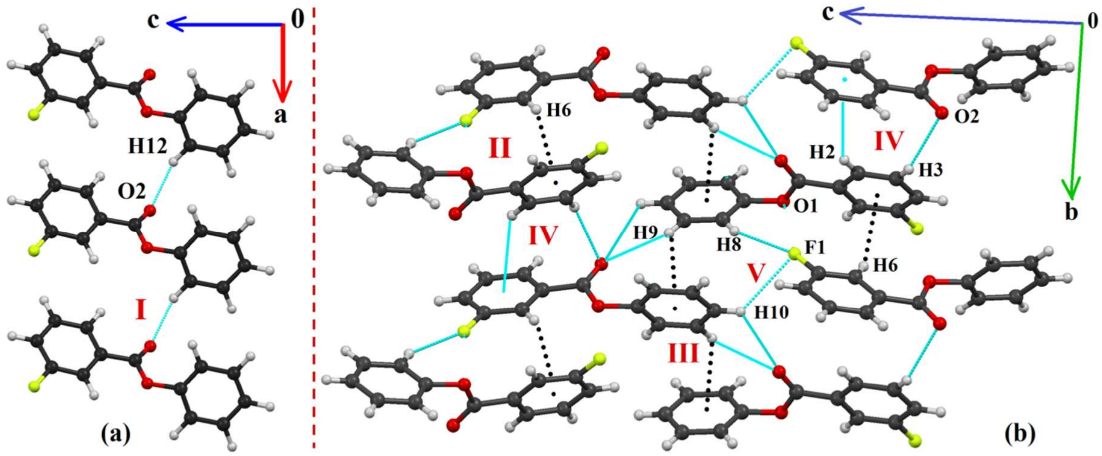

Figure 9. The packing network of D02 showing (a) 1D C-H···O chain along *a* direction; (b) the molecular sheet down the (-110) plane.

In case of D03 (space group *C*2/*c*), the molecules are connected to form a molecular sheet (**Figure 8**) down the (10-1) plane. In this molecular sheet, parallel 1D C12-H12···O2 (III; -22.1kJ/mol) chains (along the *b* direction) are connected with each other *via* C-H···F motif (involving F1 with H9, H10 and H11 and hence fluorine is a trifurcated acceptor). In addition to that, there is the formation of a chain of dimers (**Figure S27**) associated with **I** (C6-H6···O1 and C5-H5···Cg2; -26.9kJ/mol) and **V** [C3-H3···O2 and H2···H2 (1.97Å); -15.9 kJ/mol] down the (6 2 -5) plane. The chains are connected with centrosymmetric dimer II **(**C8-H8···Cg1 and C9-H9···F1; -23.7 kJ/mol**)** *via* C-H···F [VII (-4.8 kJ/mol) and VIII (-4.8 kJ/mol)] interactions. The dimers IV are connected with each other *via* π···π stacking (-17.5 kJ/mol), the centroid-centroid distance being 3.815(2) Å. The D03 has the 1D structural similarity with D22, having the high dissimilarity index of 12.3. The geometrically equivalent molecular building blocks between D03 and D22 are the D03-III/D22-III and D03-IV/D22-I (**Figures 10**, **S20a, S20c** and **S27**).

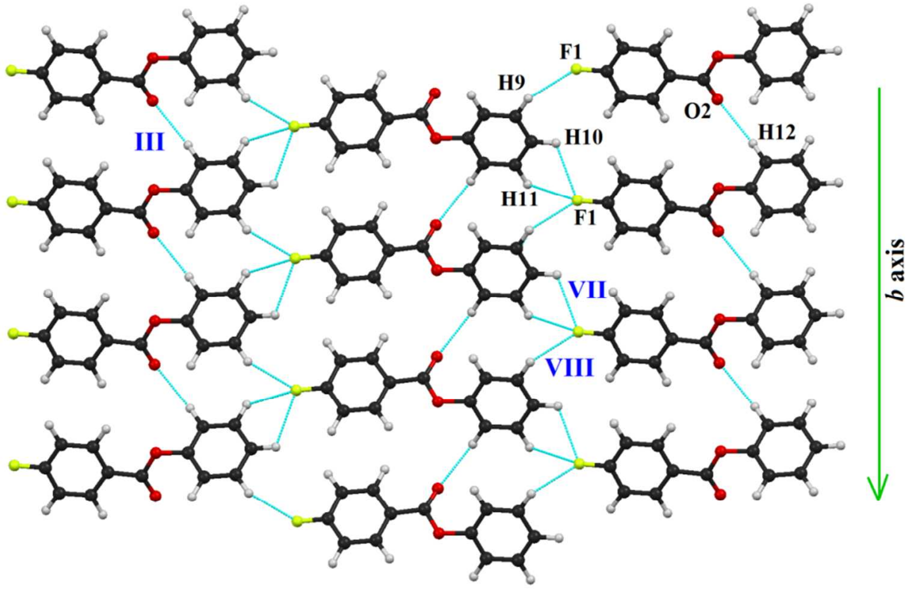

Figure 10. Crystal packing of D03 showing the molecular sheet associated with parallel C-H···O chains connected *via* trifurcated C-H···F interaction down the (10-1) plane.

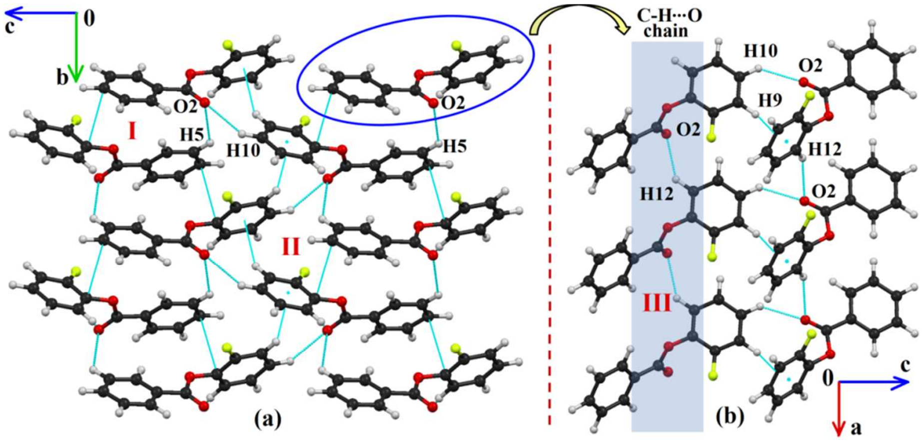

Figure 11. Crystal packing of D10 showing (a) a molecular sheet associated with C-H···O and π···π interactions down the *bc* plane, (b) 1D parallel C-H···O chains connected *via* C-H···O and C-H···π interactions down the *ac* plane.

The compound D10 crystallizes in monoclinic space group $P2_1$ with Z = 2. In this case, the molecules were found to form a molecular sheet down the *bc* plane (**Figure 11**) associated with the molecular pairs I (involving C5-H5···O2 and C4···C7 contact; -25.4 kJ/mol) and II (involving C10-H10···O2 and C9-H9···Cg2; -19.7 kJ/mol). Down the *ac* plane there is a formation of C-H···O chain involving H12 with O2 (III; -18.8 kJ/mol). Such two parallel C-H···O chains are connected with each other via the molecular pairs II and V (involving H11 with C10; -6.3kJ/mol). There is a 1D structural similarity (involving C-H···O chain) with D20 (the dissimilarity index is 9.2), D21 (the dissimilarity index is 8.9) and D31 (the dissimilarity index is 8.0). The magnitude of the dihedral angles between the two substituted benzene rings is high (> 61°) in case of D02, D10 and D22. Apart for these three structures, the dihedral angles for the other structures in this series are in the range of 52º-58º. From the studied crystal structures, it is observed that the 1D chain associated with the C-H···O interaction always occurs between C12 (*ortho* carbon of the C2 > C12 ring)-H12 and O2-C13 (these two are at opposite side of the molecular fragment C13-O1-C7-C12).

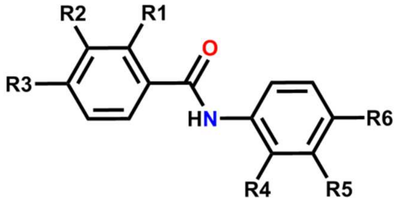

DC0: R1 = R2 = R3 = R4 = R5 = R6 = H
DC1: R1 = F, R2 = R3 = R4 = R5 = R6 = H
DC3: R3 = F, R1 = R2 = R4 = R5 = R6 = H
DC5: R5 = F, R1 = R2 = R3 = R4 = R6 = H
DC10: R1 = R5 = F, R2 = R3 = R4 = R6 = H
DC15: R3 = R6 = F, R1 = R2 = R4 = R5 = H

Scheme 2

Table 2. The lattice energies (in kJ/mol) of the FPBs and *N*-phenyl benzamides

Phenyl benzoates						*N*-phenyl benzamides					
Code	E_{Coul}	E_{Pol}	E_{Disp}	E_{Rep}	E_{Tot}	Code	E_{Coul}	E_{Pol}	E_{Disp}	E_{Rep}	E_{Tot}
D00	**-26.5**	**-10.8**	**-113.6**	**55.3**	**-95.5**	**DC0**	**-46.4**	**-22.1**	**-134.1**	**80.9**	**-121.7**
D01	**-39.3**	**-15.3**	**-129.5**	**78.3**	**-105.7**	**DC1**	**-35.9**	**-15.5**	**-120.0**	**62.8**	**-109.5**
D02	**-38.8**	**-14.7**	**-121.0**	**77.0**	**-97.5**						
D03	**-36.3**	**-15.6**	**-126.1**	**81.9**	**-96.0**	**DC3**	**-54.1**	**-20.9**	**-131.8**	**83.5**	**-123.3**
D10	**-36.3**	**-16.1**	**-123.1**	**77.1**	**-98.4**						
D20	**-36.4**	**-14.3**	**-122.6**	**76.9**	**-96.4**	**DC5**	**-50.2**	**-18.7**	**-133.9**	**79.5**	**-123.4**
D21	**-40.2**	**-14.8**	**-115.7**	**70.7**	**-99.9**	**DC10**	**-36.4**	**-17.2**	**-120.9**	**66.1**	**-108.6**
D22	**-35.1**	**-15.1**	**-119.0**	**-71.1**	**-98.2**						
D31	**-38.7**	**-15.6**	**-125.2**	**80.8**	**-98.8**						
D32	**-33.4**	**-14.1**	**-123.9**	**74.0**	**-97.4**						
D33	**-33.7**	**-14.7**	**-126.9**	**79.6**	**-95.7**	**DC15**	**-49.2**	**-18.0**	**-134.4**	**81.3**	**-120.3**

3.6. Comparison with fluorinated *N*-phenyl benzamides

The discussion is focused on the variation in molecular assembly involving the weak intermolecular interactions in the absence of any strong H-bonds. As the phenyl benzoate and their fluorinated analogues already have a strong acceptor (C=O), it is of interest to substantiate the effect due to the participation of strong donor like N-H at the position of phenoxy oxygen atom. Hence, we have compared the crystal packing features of similar type of compounds, namely *N*-phenyl benzamide [55] and their fluorinated derivatives [46, 56] [**Scheme 2** and **Table S7**] with our current study in terms of the associated nature and energetics. There is a formation of a strong N-H···O hydrogen-bonded chain along with the C-H···O interaction. It is noteworthy that 1D C-H···O chain which was already present in phenyl benzoates (strong hydrogen bond is absent), was also preserved in *N*-phenyl benzamides (**Figure S28a**). The unsubstituted *N*-phenyl benzamide (DC0) has 1D structural similarity (containing the N-H···O chain) with the unsubstituted phenyl benzoates (D00) with dissimilarity index of 15.3 (stretch parameter = 0.39Å, δa = 5.1° and δp = 14.4°). Furthermore, we have performed the *PIXEL* analysis for some selected fluorinated *N*-phenyl benzamides (**Table S8**) including the unsubstituted compound DC0. From the crystal packing analysis, it is observed that there are some similarities in the molecular arrangement between two different classes of compounds. The dihedral angle between the two benzene rings in DC0 is 62.8°, but after the addition of fluorine atom on phenyl ring, the magnitude of the dihedral angle is either drastically reduced towards planarity (DC1 and DC10) or slightly changed (DC3, DC5 and DC15). When the dihedral angle between the two substituted benzene rings is close to 0°, the intermolecular C-H···O interaction forms with a distance more than the sum of the van der Waals radii (> 2.72Å) of hydrogen and oxygen atom and with reduced directionality. Whereas, the geometry of C-H···O interaction involved in 1D chain in phenyl benzoates is totally different i.e., characterized by short H···O distance and high directionality (144°-169°). The lattice energies for all the FPBs and selected fluorinated *N*-phenyl benzamides are tabulated in **Table 2**. The comparison between two different classes of compounds having the fluorine substitution at the similar position *ortho*/*meta*/*para* is shown in **Figure S28-S29**. In most of the cases, the lattice energy of phenyl benzoates is in the range of -95.5 to -105.7 kJ/mol. The stabilization energy of the molecular pair associated with the strong N-H···O hydrogen bond and C-H···O interaction are in the range of – 41.7 to -42.5kJ/mol for DC0, DC3, DC5 and DC15. Wherein, this stabilization energy is less for DC1 (-35.9kJ/mol) and DC10 (-33.8 kJ/mol) and subsequently, the lattice energy is also less (-108 to -113 kJ/mol) compared to the other benzanilides (-120 to -124 kJ/mol). Although, DC1 and DC10 have strong H-bonds, the deviation in lattice energy is very less when compared to the respective structures (D01 and D21) with similar H/F substitution. Thus, after the launch of a strong donor (N-H) in comparison to those of phenyl benzoates, a relatively large change (-26.2 kJ/mol) in the magnitude of the lattice energy is observed.

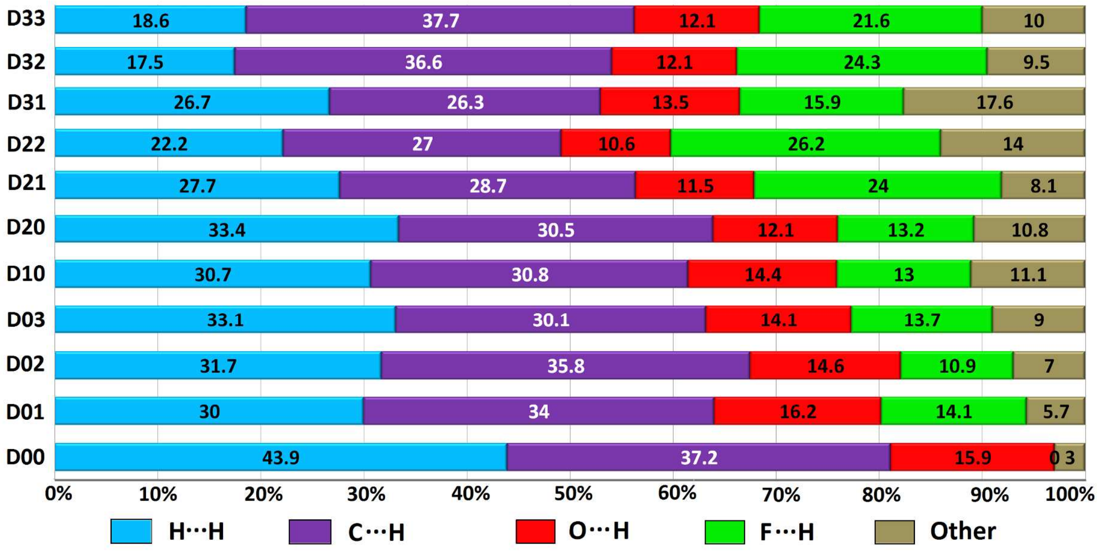

Figure 12. Relative contribution of atom···atom contacts in the crystal packing of FPBs.

3.7. Hirshfeld Surface Analysis

Hirshfeld surface analysis [57] for the FPBs was performed using the program *CrystalExplorer* 3.3 [58]. The fingerprint plots [59-60] obtained from the Hirshfeld surface analysis are shown in **Figures S30-S32**. The **Figure S30** shows the overall fingerprint plots for the 3D isostructural compounds D00-D01 and their individual atom···atom contacts (H···H, C···H, O···H and F···H). After the replacement of the aromatic hydrogen atom by the fluorine atom, the contribution for the H···H contact is drastically changed from 43.9% (D00) to 30.0% (D01). This deviation (13.9%) of the H···H contact is fulfilled by F···H contacts (14.1% in D01) *via* the formation of C-H···F intermolecular interactions. **Figure 12** represents the relative contribution of the various atom···atom contacts for phenyl benzoate and their fluorinated analogues. The contribution of the H···H contact is in the range of 30.0-33.4% and 17.5-27.7% for the mono fluoro and difluoro-substituted phenyl benzoates respectively. The contribution of C···H contacts coming from the intermolecular C-H···C interaction is in the range of 26.3-37.7%. In this case, there is no significant C-H···C contact present in the crystal packing. The H···F contact contribution is also increased for the difluorinated phenyl benzoates compared to the mono-fluoro analogues. The contribution from the intermolecular F···O contact is in the range of 0.3-2.9%. Out of eleven fluorinated crystal structures D22 (2.9%), D21 (2.1%) and D20 (2.0%) have the highest intermolecular F···O [61-62] contribution towards their individual crystal packing. The compounds D01, D10, D32 and D33 do not contain any such type of contact in the crystal lattice. Hence the fingerprint plots gives the similarities as well as the differences in terms of interatomic contacts for the two isostructural compounds (1D or 2D or 3D) as well as for the other fluorinated analogues (mono-fluoro and di-fluoro) discussed in the entire study.

4. SUMMARY

In this work, eleven crystal structures of phenyl benzoate and their fluorinated derivatives have been analyzed in terms of their molecular arrangement which exhibits isomorphism and isostructurality in the solid state. The robustness of 1D C-H···O chain plays an important role in the occurrence of isostructurality for fluorinated analogues. The molecular assembly are mainly stabilized *via* intermolecular C-H···O, C-H···F, C-H···C interaction and π···π stacking in the absence of any strong hydrogen bond. The crystal structures with 3D/2D/1D isostructurality have isoenergetic or non-isoenergetic equivalent building blocks with similar or different types of intermolecular interactions. In most of the cases, the molecular pairs with the C-H···O interaction, involved in 1D chain, are the strongest with the stabilization energy of ~ -21 kJ/mol. This quantitative investigation provides detailed physical insights into the approach of the molecules in the formation of various supramolecular construct (3D/2D/1D) in accordance with their molecular flexibility and the pattern of H/F substitution. The comparison with the fluoro substituted *N*-phenyl benzamides also provides valuable information about the occurrence of isostructurality. This is related to the method of replacement of various functional groups in the molecule. Thus, the cooperative interplay amongst the various intermolecular interactions (strong and weak) is a complex phenomenon, but the crystal environment and the flexibility associated with the weak intermolecular interactions is instrumental in the final geometrical characteristics and energetics of all the observed contacts in the crystal.

ASSOCIATED CONTENTS

Supporting Information

^{1}H-NMR Spectra, PXRD, Crystallographic refinements tables, Intermolecular interactions with the stabilization energy, Fingerprint plots from Hirshfeld surface analysis. This material is available free of charge via the Internet at http://pubs.acs.org.

ACKNOWLEDGEMENTS

D. D. thanks IISER Bhopal for the research fellowship. D. C. and D. D. thank IISER Bhopal for the research facilities, infrastructure and SERB for research funding.

AUTHOR INFORMATION

Corresponding Author

E-mail: dchopra@iiserb.ac.in. Fax: +91 755 6692392.

Notes

The authors declare no competing financial interest.

REFERENCES

1. O'Hagan, D. *Chem. Soc. Rev.* **2008**, *37*, 308–319.

2. Chopra, D. *Cryst. Growth Des*. **2012**, *12*, 541−546.

3. Reichenbacher, K.; Suss, H. I.; Hulliger, J. *Chem. Soc. Rev*. **2005**, *34*, 22−30.

4. Chopra, D; Row, T. N. G. *CrystEngComm*. **2011**, *13*, 2175-2186.

5. Mukherjee, A. *Cryst. Growth Des*. **2015**, *15*, 3076−3085.

6. Gillis, E. P.; Eastman, K. J.; Hill, M. D.; Donnelly, D. J.; Meanwell, N. A. *J. Med. Chem.* **2015**, *58*, 8315-8359.

7. Purser, S.; Moore, P. R.; Swallow, S.; Gouverneur, V. *Chem. Soc. Rev.* **2008**, *37*, 320−330.

8. Wang, J.; Sanchez-Rosello, M.; Acena, J. L.; Pozo, C. D.; Sorochinsky, A. E.; Fustero, S.; Soloshonok, V. A.; Liu, H. *Chem. Rev*. **2014**, *114*, 2432−2506.

9. Panini P.; Chopra, D. *Cryst. Growth Des.* **2014**, *14*, 3155–3168.

10. Shukla, R.; Chopra, D. *CrystEngComm*. **2015**, *17*, 3596−3609.

11. Pitts, C. R.; Siegler, M. A.; Lectka, T. *J. Org. Chem.* **2017**, *82*, 3996−4000.

12. Karnoukhova, V. A.; Fedyanin, I. V.; Lyssenko, K. A. *Struct. Chem.* **2016**, *27*, 17−44.

13. Bauza, A. and Frontera, A., *Phys. Chem. Chem. Phys.* **2016**, *18*, 20381−20388.

14. Li, P.; Maier, J. M.; Vik, E. C.; Yehl, C. J.; Dial, B. E.; Rickher, A. E.; Smith, M. D.; Pellechia, P. J.; Shimizu, K. D.; *Angew. Chem. Int. Ed*. **2017**, *56*, 1−5.

15. Schwarzer, A.; Weber, E. *Cryst. Growth Des.* **2008**, *8*, 2862−2874.

16. Saha, S.; Desiraju, G. R.; *J. Am. Chem. Soc*. **2017**, *139*, 1975−1983.

17. Desiraju, G. R. *Crystal Engineering: The Design of Organic Solids*; Elsevier: Amsterdam, 1989.

18. Kalman, A.; Parkanyi, S.; Argay, G. *Acta Crystallogr.* **1993**, *B49*, 1039−1049.

19. Fabian, L.; Kalman, A. *Acta Crystallogr.* **2004**, *B60*, 547−558.

20. Dey, D.; Chopra, D. *CrystEngComm*. **2017**, *19*, 47−63.

21. Coles, S. J.; Threlfall, T. L.; Tizzard, G. J. *Cryst. Growth Des.* **2014**, *14*, 1623−1628.

22. Esteves de Castro, R. A.; Canotilho, J.; Barbosa, R. M.; Silva, M. R.; Beja, A. M.; Paixao, J. A.; Redinha, J. S. *Cryst. Growth Des*. **2007**, *7*, 496−500.

23. Nath, K. N.; Nangia, A. *Cryst. Growth Des*. **2012**, *12*, 5411−5425.

24. Dey, D.; Thomas, S. P.; Spackman, M. A.; Chopra, D. *Chem. Commun.* **2016**, *52*, 2141−2144.

25. Mazur, L.; Koziol, A. E.; Jarzembska, K. N.; Paprocka, R.; Modzelewska-Banachiewicz, B. *Cryst. Growth Des*. **2017**, *17*, 2104−2115.

26. Suresh, K.; Khandavilli, U. B. R.; Gunnama, A. K.; Nangia, A. *CrystEngComm*. **2017**, *19*, 918–929.

27. Hutchins, K. M.; Kummer, K. A.; Groeneman, R. H.; Reinheimer, E. W.; Sinnwell, M. A.; Swensona, D. C.; MacGillivray, L. R. *CrystEngComm*. **2016**, *18*, 8354–8357.

28. Jha, K. K.; Dutta, S.; Kumar, V.; Munshi, P. *CrystEngComm*. **2016**, *18*, 8497–8505.

29. Mukherjee, A.; Desiraju, G. R. *IUCrJ*, **2014**, *1*, 49–60.

30. Turner, M. J.; Thomas, S. P.; Shi, M. W.; Jayatilaka, D.; Spackman, M. A. *Chem. Commun.* 2015, 51, 3735–3738.

31. Ebenezer, S.; Muthiah P.T.; Butcher, R. J. *Cryst. Growth Des.* **2011**, *11*, 3579–3592.

32. Capacci-Daniel, C.; Dehghan, S.; Wurster, V. M.; Basile, J. A.; Hiremath, R.; Sarjeantb, A. A.; Swift, J. A. *CrystEngComm*. **2008**, *10*, 1875–1880.

33. Patyk, E.; Podsiadło, M.; Katrusiak, A. *Cryst. Growth Des.* **2015**, *15*, 4039−4044.

34. Kumar, M.; Balaji, P. *J. Mol. Model.* **2014**, *20*, 2136.

35. Gelbrich, T.; Threlfall, T. L.; Hursthouse, M. B. *CrystEngComm*. **2012**, *14*, 5454–5464.

36. Dey, D.; Bhandary, S.; Thomas, S. P.; Spackman, M. A.; Chopra, D. *Phys. Chem. Chem. Phys.* **2016**, *18*, 31811−31820.

37. Taylor, R. *Cryst. Growth Des.* **2016**, *16*, 4165–4168.

38. Tozatti, C. S. S.; Khodyuk, R. G. D.; Silva, A. O. d.; Santos, E. d. A. d.; Dênis Pires de Lima, M. S. d. A.; Hamel, E. *Quim. Nova*, **2012**, *35*, 1758−1762.

39. Choudhury, A. R.; Winterton, N.; Steiner, A.; Cooper A. I.; Johnson, K. A., *J. Am. Chem. Soc.* **2005**, *127*, 16792−16793.

40. Dey, D.; Bhandary, S.; Sirohiwal, A.; Hathwar V. R.; Chopra, D. *Chem. Commun.* **2016**, *52*, 7225−7228.

41. Adams, J. M.; Morsi, S. E. *Acta Cryst.* **1976**, *B32*, 1345−1347.

42. Shibakami, M.; Sekiya, A. *Acta Cryst.* **1995**, *C51*, 326−330.

43. Shibakami, M.; Tamura, M.; Arimura T.; Kurosawa, S.; Sekiya, A. *Acta Cryst.* **1994**, *C50*, 592−594.

44. Farrugia, L. J. *J. Appl. Cryst.* **1999,** *32*, 837−838.

45. Nayak, S. K.; Reddy, M. K.; Chopra, D.; Row, T. N. G. *CrystEngComm*. **2012**, *14*, 200−210.

46. Chopra, D.; Row, T. N. G. *CrystEngComm*. **2008**, *10*, 54–67.

47. Dunitz, J. D.; Gavezzotti, A. *Chem. Soc. Rev.* **2009**, *38*, 2622-2633.

48. Maschio, L.; Civalleri, B.; Ugliengo, P.; Gavezzotti, A. *J. Phys. Chem. A,* **2011**, *115*, 11179-11186.

49. Gelbrich T.; Hursthouse, M. B. *CrystEngComm*. **2006**, *8*, 448–460.

50. Gelbrich, T.; Hursthouse, M. B. *CrystEngComm*. **2005**, *7*, 324–336.

51. Fabbiani, F. P. A.; Dittrich, B.; Florence, A. J.; Gelbrich, T.; Hursthouse, M. B.; Kuhs, W. F.; Shankland, N.; Sowa, H. *CrystEngComm*. **2009**, *11*, 1396−1406.

52. Mocilac, P.; Osman, I. A.; Gallagher, J. F. *CrystEngComm.* **2016**, *18*, 5764–5776.

53. Burgi H.; Dunitz, J.; Lehn, J.; Wipff, G. *Tetrahedron*, **1974**, *30*, 1563-1572.

54. Battle, G. M.; Ferrence, G. M.; Allen, F. H. *J. Appl. Cryst*. **2010**, *43*, 1208-1223.

55. Wang, J. –L.; Xu, J. –S.; Wang, D. –Y.; Wang, H.; Li, Z. –T.; Zhang, D. –W. *CrystEngComm*. **2014**, *16*, 2078-2084.

56. Chopra, D.; Row, T. N. G. *Cryst.Growth Des*. **2005**, *5*, 1679−1681.

57. Spackman, M. A.; D. Jayatilaka, *CrystEngComm*. **2009**, *11*, 19−32.

58. Wolff, S. K.; Grimwood, D. J.; McKinnon, J. J.; Turner, M. J.; Jayatilaka, D.; Spackman, M. A. *CrystalExplorer, Version 3.1*; University of Western Australia: Crawley, Australia, 2012.

59. Spackman M. A.; Mckinnon, J. J. *CrystEngComm*. **2002**, *4*, 378−392.

60. Mckinnon, J. J.; Jayatilaka, D.; Spackman, M. A. *Chem. Commun.* **2007**, 3814−3816.

61. Sirohiwal, A.; Hathwar, V. R.; Dey, D.; Regunathan, R.; Chopra, D. *Acta Cryst*. **2017**, *B73*, 140−152.

62. Jelsch, C.; Guillot, B. *Acta Cryst*. **2017**, *B73*, 136–137.

For Table of Contents Use Only:

Manuscript title: Evaluation of the role of isostructurality in fluorinated phenyl benzoates

Authors: Dhananjay Dey and Deepak Chopra

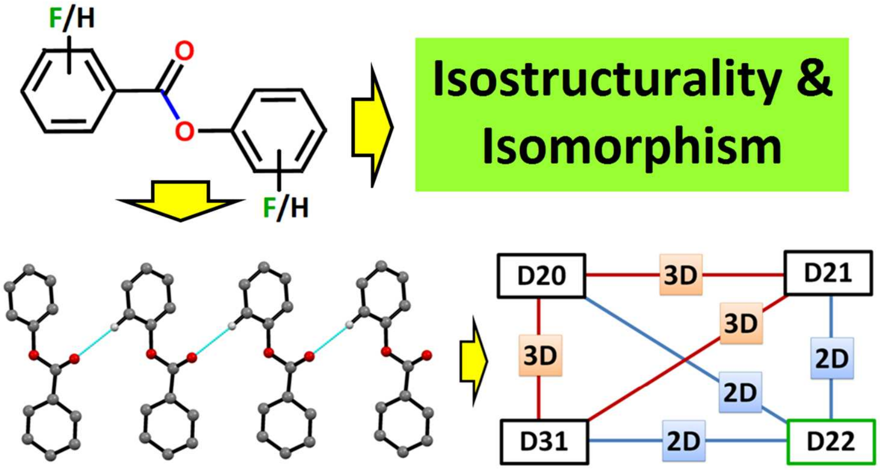

Synopsis

In this study, a total of eleven crystal structures of isomeric fluorinated phenyl benzoates have been analyzed in terms of their molecular arrangement which exhibits the phenomenon of isomorphism and isostructurality. The 1D C-H···O=C chain is observed as a robust motif and plays an important role in the occurrence of isostructurality.